

Measurement of the ratio $\mathcal{B}(D^0 \rightarrow \pi^+\pi^-\pi^0)/\mathcal{B}(D^0 \rightarrow K^-\pi^+\pi^0)$

K. Abe,⁹ K. Abe,⁴⁹ I. Adachi,⁹ H. Aihara,⁵¹ D. Anipko,¹ K. Aoki,²⁵ T. Arakawa,³²
 K. Arinstein,¹ Y. Asano,⁵⁶ T. Aso,⁵⁵ V. Aulchenko,¹ T. Aushev,²¹ T. Aziz,⁴⁷ S. Bahinipati,⁴
 A. M. Bakich,⁴⁶ V. Balagura,¹⁵ Y. Ban,³⁷ S. Banerjee,⁴⁷ E. Barberio,²⁴ M. Barbero,⁸
 A. Bay,²¹ I. Bedny,¹ K. Belous,¹⁴ U. Bitenc,¹⁶ I. Bizjak,¹⁶ S. Blyth,²⁷ A. Bondar,¹
 A. Bozek,³⁰ M. Bračko,^{23,16} J. Brodzicka,^{9,30} T. E. Browder,⁸ M.-C. Chang,⁵⁰ P. Chang,²⁹
 Y. Chao,²⁹ A. Chen,²⁷ K.-F. Chen,²⁹ W. T. Chen,²⁷ B. G. Cheon,³ R. Chistov,¹⁵
 J. H. Choi,¹⁸ S.-K. Choi,⁷ Y. Choi,⁴⁵ Y. K. Choi,⁴⁵ A. Chuvikov,³⁹ S. Cole,⁴⁶ J. Dalseno,²⁴
 M. Danilov,¹⁵ M. Dash,⁵⁷ R. Dowd,²⁴ J. Dragic,⁹ A. Drutskey,⁴ S. Eidelman,¹ Y. Enari,²⁵
 D. Epifanov,¹ S. Fratina,¹⁶ H. Fujii,⁹ M. Fujikawa,²⁶ N. Gabyshev,¹ A. Garmash,³⁹
 T. Gershon,⁹ A. Go,²⁷ G. Gokhroo,⁴⁷ P. Goldenzweig,⁴ B. Golob,^{22,16} A. Gorišek,¹⁶
 M. Grosse Perdekamp,^{11,40} H. Guler,⁸ H. Ha,¹⁸ J. Haba,⁹ K. Hara,²⁵ T. Hara,³⁵
 Y. Hasegawa,⁴⁴ N. C. Hastings,⁵¹ K. Hayasaka,²⁵ H. Hayashii,²⁶ M. Hazumi,⁹
 D. Heffernan,³⁵ T. Higuchi,⁹ L. Hinz,²¹ T. Hokuue,²⁵ Y. Hoshi,⁴⁹ K. Hoshina,⁵⁴ S. Hou,²⁷
 W.-S. Hou,²⁹ Y. B. Hsiung,²⁹ Y. Igarashi,⁹ T. Iijima,²⁵ K. Ikado,²⁵ A. Imoto,²⁶ K. Inami,²⁵
 A. Ishikawa,⁵¹ H. Ishino,⁵² K. Itoh,⁵¹ R. Itoh,⁹ M. Iwabuchi,⁶ M. Iwasaki,⁵¹ Y. Iwasaki,⁹
 C. Jacoby,²¹ M. Jones,⁸ H. Kakuno,⁵¹ J. H. Kang,⁵⁸ J. S. Kang,¹⁸ P. Kapusta,³⁰
 S. U. Kataoka,²⁶ N. Katayama,⁹ H. Kawai,² T. Kawasaki,³² H. R. Khan,⁵² A. Kibayashi,⁵²
 H. Kichimi,⁹ N. Kikuchi,⁵⁰ H. J. Kim,²⁰ H. O. Kim,⁴⁵ J. H. Kim,⁴⁵ S. K. Kim,⁴³
 T. H. Kim,⁵⁸ Y. J. Kim,⁶ K. Kinoshita,⁴ N. Kishimoto,²⁵ S. Korpar,^{23,16} Y. Kozakai,²⁵
 P. Križan,^{22,16} P. Krokovny,⁹ T. Kubota,²⁵ R. Kulasiri,⁴ R. Kumar,³⁶ C. C. Kuo,²⁷
 E. Kurihara,² A. Kusaka,⁵¹ A. Kuzmin,¹ Y.-J. Kwon,⁵⁸ J. S. Lange,⁵ G. Leder,¹³ J. Lee,⁴³
 S. E. Lee,⁴³ Y.-J. Lee,²⁹ T. Lesiak,³⁰ J. Li,⁸ A. Limosani,⁹ C. Y. Lin,²⁹ S.-W. Lin,²⁹
 Y. Liu,⁶ D. Liventsev,¹⁵ J. MacNaughton,¹³ G. Majumder,⁴⁷ F. Mandl,¹³ D. Marlow,³⁹
 T. Matsumoto,⁵³ A. Matyja,³⁰ S. McOnie,⁴⁶ T. Medvedeva,¹⁵ Y. Mikami,⁵⁰ W. Mitaroff,¹³
 K. Miyabayashi,²⁶ H. Miyake,³⁵ H. Miyata,³² Y. Miyazaki,²⁵ R. Mizuk,¹⁵ D. Mohapatra,⁵⁷
 G. R. Moloney,²⁴ T. Mori,⁵² J. Mueller,³⁸ A. Murakami,⁴¹ T. Nagamine,⁵⁰ Y. Nagasaka,¹⁰
 T. Nakagawa,⁵³ Y. Nakahama,⁵¹ I. Nakamura,⁹ E. Nakano,³⁴ M. Nakao,⁹ H. Nakazawa,⁹
 Z. Natkaniec,³⁰ K. Neichi,⁴⁹ S. Nishida,⁹ K. Nishimura,⁸ O. Nitoh,⁵⁴ S. Noguchi,²⁶
 T. Nozaki,⁹ A. Ogawa,⁴⁰ S. Ogawa,⁴⁸ T. Ohshima,²⁵ T. Okabe,²⁵ S. Okuno,¹⁷ S. L. Olsen,⁸
 S. Ono,⁵² W. Ostrowicz,³⁰ H. Ozaki,⁹ P. Pakhlov,¹⁵ G. Pakhlova,¹⁵ H. Palka,³⁰
 C. W. Park,⁴⁵ H. Park,²⁰ K. S. Park,⁴⁵ N. Parslow,⁴⁶ L. S. Peak,⁴⁶ M. Pernicka,¹³
 R. Pestotnik,¹⁶ M. Peters,⁸ L. E. Piilonen,⁵⁷ A. Poluektov,¹ F. J. Ronga,⁹ N. Root,¹
 J. Rorie,⁸ M. Rozanska,³⁰ H. Sahoo,⁸ S. Saitoh,⁹ Y. Sakai,⁹ H. Sakamoto,¹⁹ H. Sakaue,³⁴
 T. R. Sarangi,⁶ N. Sato,²⁵ N. Satoyama,⁴⁴ K. Sayeed,⁴ T. Schietinger,²¹ O. Schneider,²¹
 P. Schönmeier,⁵⁰ J. Schümann,²⁸ C. Schwanda,¹³ A. J. Schwartz,⁴ R. Seidl,^{11,40} T. Seki,⁵³
 K. Senyo,²⁵ M. E. Sevier,²⁴ M. Shapkin,¹⁴ Y.-T. Shen,²⁹ H. Shibuya,⁴⁸ B. Shwartz,¹
 V. Sidorov,¹ J. B. Singh,³⁶ A. Sokolov,¹⁴ A. Somov,⁴ N. Soni,³⁶ R. Stamen,⁹ S. Stanič,³³
 M. Starič,¹⁶ H. Stoeck,⁴⁶ A. Sugiyama,⁴¹ K. Sumisawa,⁹ T. Sumiyoshi,⁵³ S. Suzuki,⁴¹
 S. Y. Suzuki,⁹ O. Tajima,⁹ N. Takada,⁴⁴ F. Takasaki,⁹ K. Tamai,⁹ N. Tamura,³²
 K. Tanabe,⁵¹ M. Tanaka,⁹ G. N. Taylor,²⁴ Y. Teramoto,³⁴ X. C. Tian,³⁷ I. Tikhomirov,¹⁵

K. Trabelsi,⁹ Y. T. Tsai,²⁹ Y. F. Tse,²⁴ T. Tsuboyama,⁹ T. Tsukamoto,⁹ K. Uchida,⁸
Y. Uchida,⁶ S. Uehara,⁹ T. Uglov,¹⁵ K. Ueno,²⁹ Y. Unno,⁹ S. Uno,⁹ P. Urquijo,²⁴
Y. Ushiroda,⁹ Y. Usov,¹ G. Varner,⁸ K. E. Varvell,⁴⁶ S. Villa,²¹ C. C. Wang,²⁹
C. H. Wang,²⁸ M.-Z. Wang,²⁹ M. Watanabe,³² Y. Watanabe,⁵² J. Wicht,²¹ L. Widhalm,¹³
J. Wiechczynski,³⁰ E. Won,¹⁸ C.-H. Wu,²⁹ Q. L. Xie,¹² B. D. Yabsley,⁴⁶ A. Yamaguchi,⁵⁰
H. Yamamoto,⁵⁰ S. Yamamoto,⁵³ Y. Yamashita,³¹ M. Yamauchi,⁹ Heyoung Yang,⁴³
S. Yoshino,²⁵ Y. Yuan,¹² Y. Yusa,⁵⁷ S. L. Zang,¹² C. C. Zhang,¹² J. Zhang,⁹
L. M. Zhang,⁴² Z. P. Zhang,⁴² V. Zhilich,¹ T. Ziegler,³⁹ A. Zupanc,¹⁶ and D. Zürcher²¹

(The Belle Collaboration)

(Belle Collaboration)

¹*Budker Institute of Nuclear Physics, Novosibirsk*

²*Chiba University, Chiba*

³*Chonnam National University, Kwangju*

⁴*University of Cincinnati, Cincinnati, Ohio 45221*

⁵*University of Frankfurt, Frankfurt*

⁶*The Graduate University for Advanced Studies, Hayama*

⁷*Gyeongsang National University, Chinju*

⁸*University of Hawaii, Honolulu, Hawaii 96822*

⁹*High Energy Accelerator Research Organization (KEK), Tsukuba*

¹⁰*Hiroshima Institute of Technology, Hiroshima*

¹¹*University of Illinois at Urbana-Champaign, Urbana, Illinois 61801*

¹²*Institute of High Energy Physics,*

Chinese Academy of Sciences, Beijing

¹³*Institute of High Energy Physics, Vienna*

¹⁴*Institute of High Energy Physics, Protvino*

¹⁵*Institute for Theoretical and Experimental Physics, Moscow*

¹⁶*J. Stefan Institute, Ljubljana*

¹⁷*Kanagawa University, Yokohama*

¹⁸*Korea University, Seoul*

¹⁹*Kyoto University, Kyoto*

²⁰*Kyungpook National University, Taegu*

²¹*Swiss Federal Institute of Technology of Lausanne, EPFL, Lausanne*

²²*University of Ljubljana, Ljubljana*

²³*University of Maribor, Maribor*

²⁴*University of Melbourne, Victoria*

²⁵*Nagoya University, Nagoya*

²⁶*Nara Women's University, Nara*

²⁷*National Central University, Chung-li*

²⁸*National United University, Miao Li*

²⁹*Department of Physics, National Taiwan University, Taipei*

³⁰*H. Niewodniczanski Institute of Nuclear Physics, Krakow*

³¹*Nippon Dental University, Niigata*

³²*Niigata University, Niigata*

³³*University of Nova Gorica, Nova Gorica*

³⁴*Osaka City University, Osaka*

- ³⁵*Osaka University, Osaka*
³⁶*Panjab University, Chandigarh*
³⁷*Peking University, Beijing*
³⁸*University of Pittsburgh, Pittsburgh, Pennsylvania 15260*
³⁹*Princeton University, Princeton, New Jersey 08544*
⁴⁰*RIKEN BNL Research Center, Upton, New York 11973*
⁴¹*Saga University, Saga*
⁴²*University of Science and Technology of China, Hefei*
⁴³*Seoul National University, Seoul*
⁴⁴*Shinshu University, Nagano*
⁴⁵*Sungkyunkwan University, Suwon*
⁴⁶*University of Sydney, Sydney NSW*
⁴⁷*Tata Institute of Fundamental Research, Bombay*
⁴⁸*Toho University, Funabashi*
⁴⁹*Tohoku Gakuin University, Tagajo*
⁵⁰*Tohoku University, Sendai*
⁵¹*Department of Physics, University of Tokyo, Tokyo*
⁵²*Tokyo Institute of Technology, Tokyo*
⁵³*Tokyo Metropolitan University, Tokyo*
⁵⁴*Tokyo University of Agriculture and Technology, Tokyo*
⁵⁵*Toyama National College of Maritime Technology, Toyama*
⁵⁶*University of Tsukuba, Tsukuba*
⁵⁷*Virginia Polytechnic Institute and State University, Blacksburg, Virginia 24061*
⁵⁸*Yonsei University, Seoul*

Abstract

We report a high-statistics measurement of the relative branching fraction $\mathcal{B}(D^0 \rightarrow \pi^+\pi^-\pi^0)/\mathcal{B}(D^0 \rightarrow K^-\pi^+\pi^0)$. A 357 fb^{-1} data sample collected with the Belle detector at the KEKB asymmetric-energy e^+e^- collider was used for the analysis. The relative branching fraction $\mathcal{B}(D^0 \rightarrow \pi^+\pi^-\pi^0)/\mathcal{B}(D^0 \rightarrow K^-\pi^+\pi^0)$ is determined with an accuracy comparable to the latest world average value.

PACS numbers: 13.25.Ft, 14.40.Lb

INTRODUCTION

This measurement is the first step towards a high-statistics Dalitz-plot analysis of the $D^0 \rightarrow \pi^+\pi^-\pi^0$ decay. The latter could give insight into the controversy on the S-wave $\pi^+\pi^-$ contribution in these decays [1, 2], as well as a sensitive study of the CP violation in the neutral D meson system. Knowledge of $\mathcal{B}(D^0 \rightarrow \rho\pi)/\mathcal{B}(D^0 \rightarrow K^*K)$ (also based on the $D^0 \rightarrow \pi^+\pi^-\pi^0$ Dalitz analysis) could improve our understanding of the apparent discrepancy of the measured two-body branching fractions ($D^0 \rightarrow KK, \pi\pi$) with the theoretical expectations [3]. The accuracy of the value of $\mathcal{B}(D^0 \rightarrow \pi^+\pi^-\pi^0)$ as reported in PDG04 [4] is poor. Using a large data sample of D^0 decays accumulated with the Belle detector, we provide a significantly improved measurement using the $D^0 \rightarrow K^-\pi^+\pi^0$ decay mode for normalization. Since both decay modes involve a neutral pion and the same number of charged tracks in the final state, several sources of the systematic uncertainties are avoided in a determination of the relative branching fraction. The obtained result can then be compared to recent measurements by the CLEO [5] and BABAR [6] collaborations. A detailed study of the $D^0 \rightarrow \pi^+\pi^-\pi^0$ decay as well as of other D^0 CP -symmetric final states, can be used to further improve statistics for the measurement of the angle ϕ_3 (γ) of the CKM-matrix.

EXPERIMENT

The Belle detector is a large-solid-angle magnetic spectrometer located at the KEKB e^+e^- storage rings, which collide 8.0 GeV electrons with 3.5 GeV positrons and produce $\Upsilon(4S)$ at the energy of 10.58 GeV. Closest to the interaction point is a silicon vertex detector (SVD), surrounded by a 50-layer central drift chamber (CDC), an array of aerogel Cherenkov counters (ACC), a barrel-like arrangement of time-of-flight (TOF) scintillation counters, and an electromagnetic calorimeter (ECL) comprised of CsI (Tl) crystals. These subdetectors are located inside a superconducting solenoid coil that provides a 1.5 T magnetic field. An iron flux-return yoke located outside the coil is instrumented to detect K_L^0 mesons and identify muons. The detector is described in detail elsewhere [7, 8].

DATA SELECTION

For this analysis, we used a data sample of 357 fb $^{-1}$ accumulated with the Belle detector. D^0 candidates are selected from $D^* \rightarrow D^0\pi_{\text{slow}}$ decays where the charge of the π_{slow} tags the D^0 flavour: $D^{*\pm} \rightarrow D^0/\overline{D^0}\pi_{\text{slow}}^\pm$. D^* 's originate mainly from continuum. Although we do not apply any topological cuts, the yield of D^* 's from B -meson decays is negligible; such events are rejected by other kinematical cuts such as the strong $p_{\text{cms}}(D^*)$ requirement. D^0 mesons are reconstructed from combinations of two oppositely charged pions (or a charged pion and kaon in the case of $K^-\pi^+\pi^0$) and one neutral pion. The latter is reconstructed from two γ candidates satisfying the π^0 mass requirement given below.

The following kinematic criteria are applied to the charged track candidates: the distance from the nominal interaction point to the point of closest approach of the track is required to be within 0.15 cm in the radial direction (dr) and 0.3 cm along the beam direction (dz).

We also require the transverse momentum of the track $p_{\perp} > 0.050$ GeV/c to suppress beam background. Kaons and pions are separated by combining the responses of the ACC and the TOF with the dE/dx measurement from the CDC to form a likelihood $\mathcal{L}(h)$ where h is a pion or a kaon. Charged particles are identified as pions or kaons using the likelihood ratio $\mathcal{R}_{\text{PID}} = \mathcal{L}(K)/(\mathcal{L}(K) + \mathcal{L}(\pi))$. For charged pion identification, we require $\mathcal{R}_{\text{PID}} < 0.4$. This requirement selects pions with an efficiency of 93% and misidentified kaons with an efficiency of 9%. For the identification of charged kaons, the requirement is $\mathcal{R}_{\text{PID}} > 0.6$; in this case, the efficiency for kaon identification is 86% and the probability to misidentify a pion is 4%.

We impose conditions on the energies of the photons constituting the π^0 candidate ($E_{\gamma}(\pi^0) > 0.060$ GeV), the two-photon invariant mass ($0.124 \text{ GeV}/c^2 < M(\gamma\gamma) < 0.148 \text{ GeV}/c^2$) and the π^0 's momentum in the laboratory frame ($p_{\text{lab}}(\pi^0) > 0.3 \text{ GeV}/c$) to suppress combinatorial π^0 's.

The mass difference of D^* and D^0 candidates should satisfy the restrictions: $0.1442 \text{ GeV}/c^2 < M(\pi_{\text{slow}}\pi^+\pi^-\pi^0) - M(\pi^+\pi^-\pi^0) < 0.1468 \text{ GeV}/c^2$ and $0.1440 \text{ GeV}/c^2 < M(\pi_{\text{slow}}K^-\pi^+\pi^0) - M(K^-\pi^+\pi^0) < 0.1470 \text{ GeV}/c^2$. The momentum of the D^* in the center-of-mass frame of the $\Upsilon(4S)$ must lie in the range: $3.5 \text{ GeV}/c < p_{\text{cms}}(D^*) < 4.3 \text{ GeV}/c$. The lower cut is applied to suppress slow fake D^* 's reconstructed from combinatorial background that originates from B decays. The upper cut restricts $p_{\text{cms}}(D^*)$ to the region where the Monte Carlo (MC) distribution is in good agreement with the data (see Fig. 1, left). To eliminate background from the $D^0 \rightarrow K_S\pi^0 \rightarrow (\pi^+\pi^-)\pi^0$ decays, the following veto on $M^2(\pi^+\pi^-)$ is applied: $0.21 \text{ GeV}^2/c^4 < M^2(\pi^+\pi^-) < 0.29 \text{ GeV}^2/c^4$.

EFFICIENCY CALCULATION

To obtain detection efficiencies, about 1.2×10^6 phase-space distributed MC events have been generated for each of the two modes, processed using the GEANT-based detector simulation [9] and reconstructed with the same selection criteria as the data.

To obtain a more realistic D^0 decay model than a uniform Dalitz-plot distribution, the events of both signal MC samples have been weighted using matrix elements based on decay models obtained by CLEO [1] in the framework of a 3-resonance model (ρ^+ , ρ^- , ρ^0 and a nonresonant contribution) for $D^0 \rightarrow \pi^+\pi^-\pi^0$ and in the framework of a 7-resonance model (ρ^+ , K^{*-} , \bar{K}^{*0} , $K_0(1430)^-$, $\bar{K}_0(1430)^0$, $\rho(1700)^+$, $K^{*-}(1680)$ and a nonresonant contribution) for the case of $D^0 \rightarrow K^-\pi^+\pi^0$ [10] (see Fig. 2).

The obtained yield is normalized to the same MC data but before detector simulation and before application of selection criteria. Since for the relative branching fraction measurement only the ratio of $\pi^+\pi^-\pi^0$ and $K^-\pi^+\pi^0$ efficiencies is needed, we only generate events in the $p_{\text{cms}}(D^*)$ range from 3.5 to 4.3 GeV/c where MC is in good agreement with the data (see Fig. 1, left). The obtained efficiencies are: $\varepsilon(\pi^+\pi^-\pi^0) = (13.433 \pm 0.077)\%$, $\varepsilon(K^-\pi^+\pi^0) = (13.065 \pm 0.074)\%$.

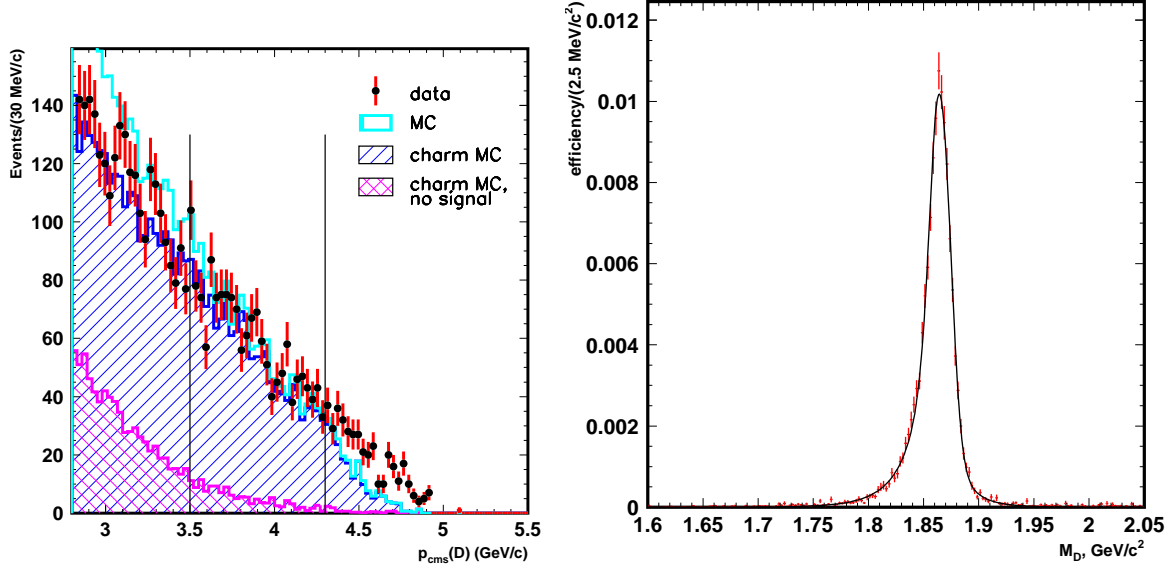


FIG. 1: Left: $p_{\text{cms}}(D^*)$ distribution for experimental data (points with error bars), generic MC (solid line), charm (originating from $e^+e^- \rightarrow c\bar{c}$) MC including signal events (singly hatched histogram) and background charm MC (doubly hatched histogram). Right: $M(\pi^+\pi^-\pi^0)$ distribution, MC, fitted with a bifurcated hyperbolic Gaussian and a regular Gaussian.

BACKGROUND DESCRIPTION

To describe the background shape in the $M(\pi^+\pi^-\pi^0)$ signal region, a sample of generic MC, equivalent to $\sim 250 \text{ fb}^{-1}$, has been processed with the same selection criteria as data. The contributions of $u\bar{u}$, $d\bar{d}$, $s\bar{s}$, $c\bar{c}$ and $B\bar{B}$ backgrounds have been summed up. For the $c\bar{c}$ sample signal events were excluded. Figure 3 shows the individual contributions to the $M(\pi^+\pi^-\pi^0)$ distribution where also a partial data sample, corresponding to the luminosity of MC, is shown. The $M(\pi^+\pi^-\pi^0)$ background distribution is fitted with a 2^{nd} order polynomial multiplied by an error function (kaon misidentification region) plus a 1^{st} order polynomial (combinatoric background) and a small Gaussian peak in the signal region (see Fig. 3, right). The Gaussian contribution is mainly due to combinations of a correctly reconstructed D^0 and a random π_{slow} candidate.

Most of the background is from $e^+e^- \rightarrow c\bar{c}$; the $B\bar{B}$ background is negligible and $u\bar{u}$, $d\bar{d}$, $s\bar{s}$ backgrounds are linearly distributed in the $M(\pi^+\pi^-\pi^0)$ signal region. Among the $c\bar{c}$ background sources $D^* \rightarrow D^0(K\pi\pi^0)\pi$ is dominant: charged kaons are misidentified as pions and $M(\pi_{\text{fake}}\pi\pi^0)$ is typically shifted downwards by $\sim 0.1 \text{ GeV}/c^2$ thus being well separated from the signal.

The background shape in the $M(K^-\pi^+\pi^0)$ distribution is obtained using a generic MC sample. The level of background in this mode is low but still has a nontrivial structure (see Fig. 4, right). The distribution has three distinctive peaks: the rightmost one is due to misidentified pions from $D^0 \rightarrow \pi^+\pi^-\pi^0$, the central one has the same origin as the one in the $D^0 \rightarrow \pi^+\pi^-\pi^0$ case (random π_{slow}), the leftmost feature originates mainly from

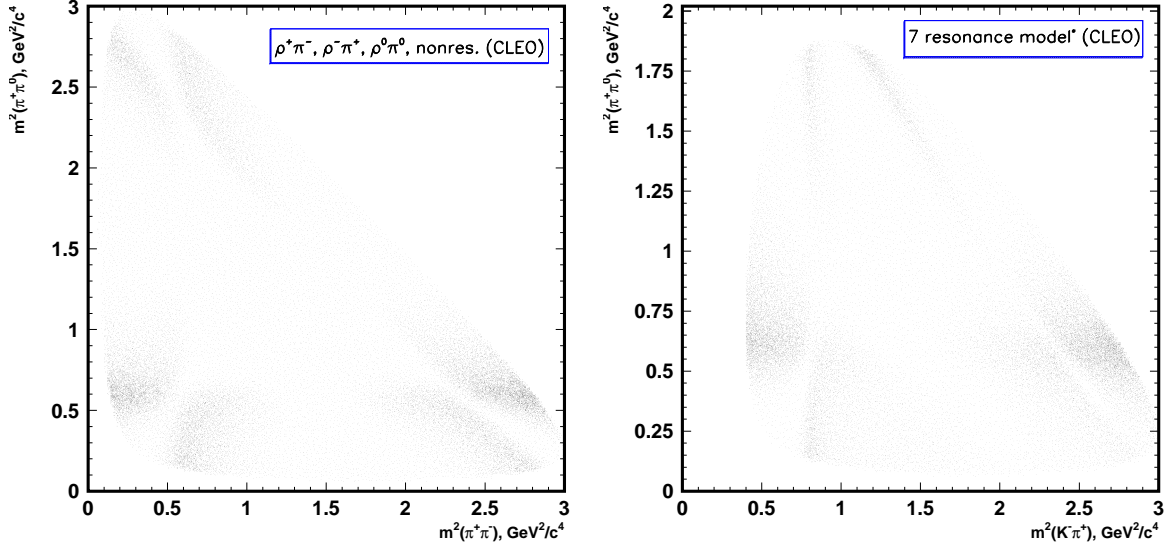


FIG. 2: Dalitz plot distribution for "initial" signal MC (before skimming and detector simulation) in the $D^0 \rightarrow \pi^+\pi^-\pi^0$ (left, 3-resonance model) and $D^0 \rightarrow K^-\pi^+\pi^0$ (right, 7-resonance model) cases.

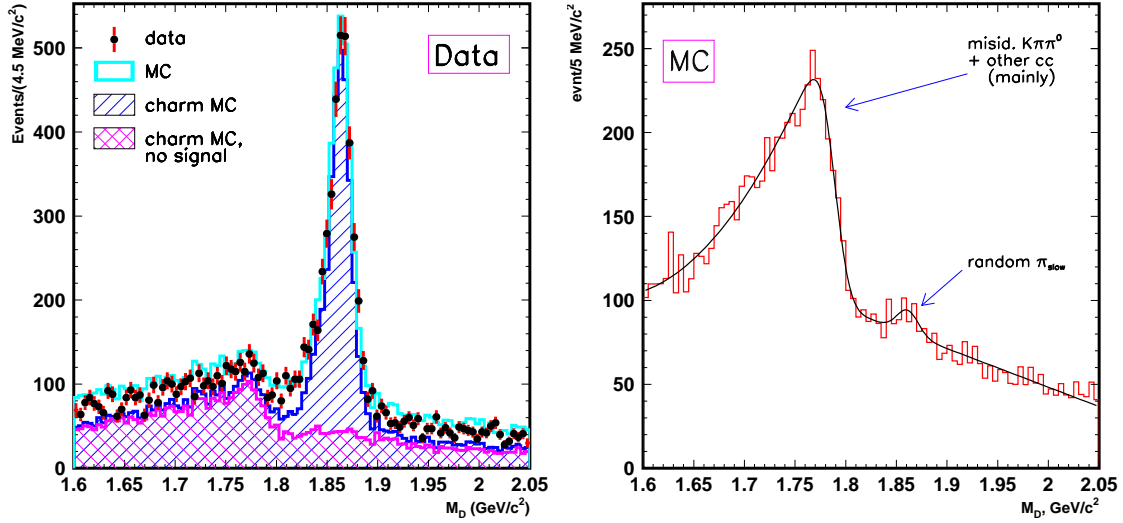


FIG. 3: Left: $M(\pi^+\pi^-\pi^0)$ distribution for experimental data (points with error bars), generic MC (solid line), charm (originating from $e^+e^- \rightarrow c\bar{c}$) MC including signal events (singly hatched histogram) and background charm MC (doubly hatched histogram). Right: $M(\pi^+\pi^-\pi^0)$, "charm" MC with the signal excluded, fitted to the function described in the text.

$D^0 \rightarrow Kn\pi$ where $n \geq 3$. The distribution is fitted by the sum of a 2^{nd} order polynomial and a 2^{nd} order polynomial multiplied by an error function (left peak) and two Gaussians.

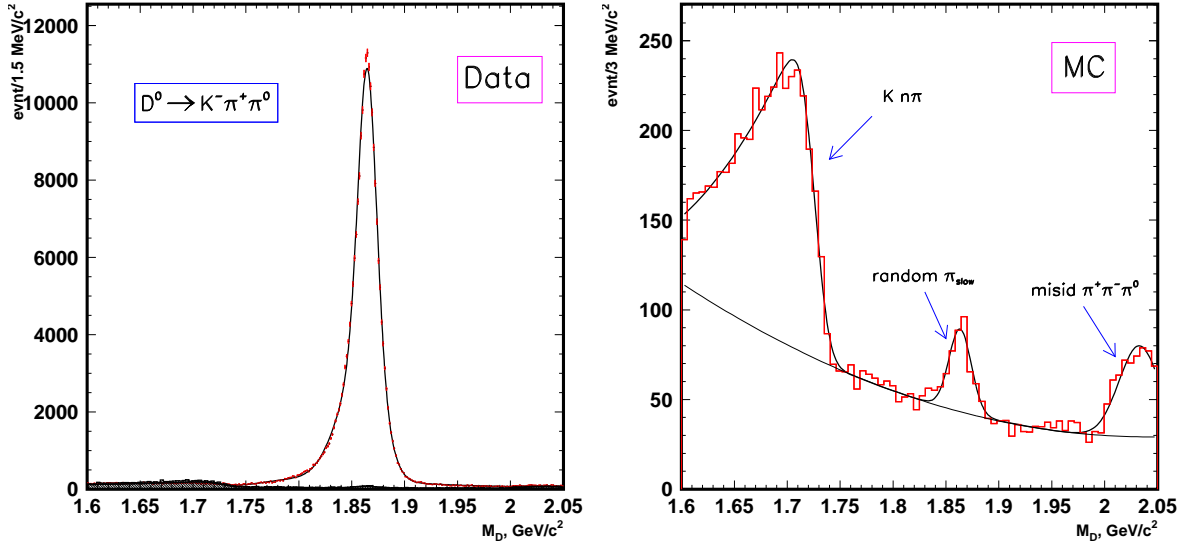


FIG. 4: Left: signal $M(K\pi\pi^0)$ distribution fitted with 2 bifurcated Gaussians + Gaussian (signal peak) and the generic MC shape (background). Right: background shape $M(K\pi\pi^0)$, generic MC.

SIGNAL FIT

The shape of the signal peak in the experimental $\pi^+\pi^-\pi^0$ invariant mass distribution (see Fig. 5, left) is partially fixed to the MC one [13]: the latter was fitted with a bifurcated hyperbolic Gaussian [14, 15] and a regular Gaussian (see Fig. 1, right). The obtained shape with floating normalization and σ 's, together with the background shape with its floating normalization (i.e. 5 free parameters) is then used as the fit function for the measured $M(\pi^+\pi^-\pi^0)$ distribution.

To fit the experimental $K\pi\pi^0$ invariant mass distribution we use a $K\pi\pi^0$ background shape with floating normalization and the sum of two bifurcated and a regular Gaussian for the signal peak (see Fig. 4, right). Here, the parameters of the signal peak are free in the fit since the level of background is low and statistics are large enough.

The yields of signal events in each channel, as obtained from the fit, are given in Table I:

TABLE I: Number of signal events and efficiencies

D^0 decay mode	N_{ev}	$\varepsilon, \%$
$\pi^+\pi^-\pi^0$	22803 ± 203	13.433 ± 0.077
$K^-\pi^+\pi^0$	237520 ± 500	13.065 ± 0.074

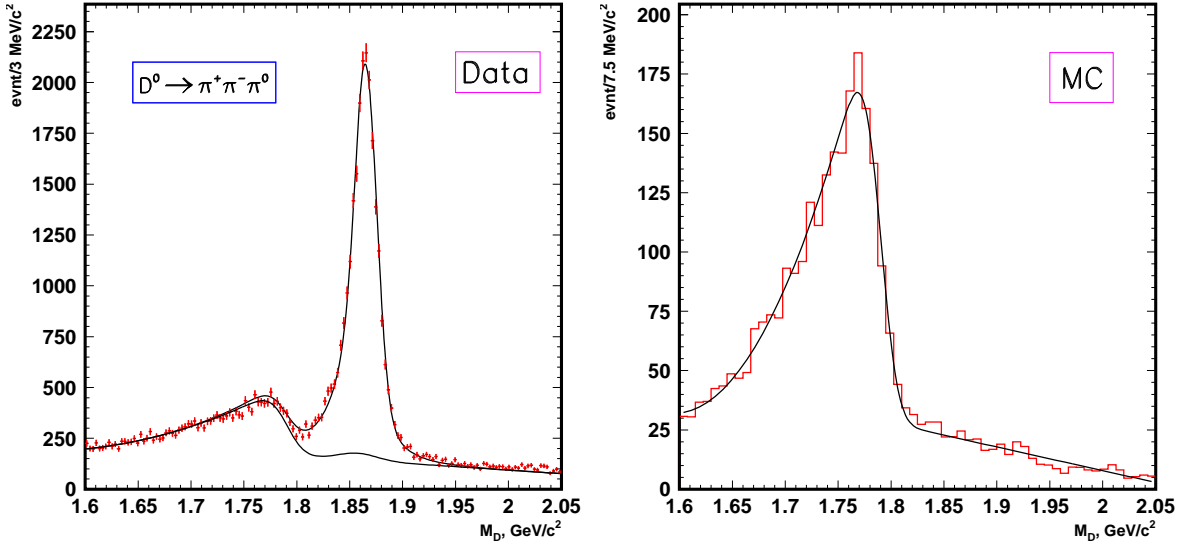


FIG. 5: Left: signal $M(\pi^+\pi^-\pi^0)$ distribution, fitted to the signal MC shape (Fig. 1, right) for the signal peak and with the generic MC shape (background). Right: misidentification shape, generic MC, used for an alternative background fit to estimate the corresponding systematic error.

SYSTEMATIC UNCERTAINTIES

Uncertainty on the tracking efficiency for the two charged tracks - $\pi^+\pi^-$ or $K^-\pi^+$ - cancels in the ratio of $D^0 \rightarrow \pi^+\pi^-\pi^0$ and $D^0 \rightarrow K^-\pi^+\pi^0$ branching fractions. The same holds for π^0 and slow pion (from D^*) reconstruction efficiencies. A possible difference in the efficiency of particle identification selection criteria between MC and data is taken into account as a correction to the branching ratio ($r_K/r_\pi = 0.962 \pm 0.015$) and the uncertainty of this correction contributes to the systematic uncertainty of the result. The polar angle and momentum dependent data/MC corrections are measured independently using a large sample of $D^0 \rightarrow K^-\pi^+$ decays. The uncertainty in the correction yields a systematic error of 1.6%.

To estimate the systematic error due to the model used to describe the $D^0 \rightarrow \pi^+\pi^-\pi^0$ decay, we have compared MC efficiencies using the two different models mentioned above: the one obtained by CLEO [1] (used in the final result for the branching ratio) and the same model but without interference: only the branching fractions of the intermediate resonances have been taken into account. Both models consider three intermediate resonances (ρ^+ , ρ^- , ρ^0 and a nonresonant contribution).

For the $D^0 \rightarrow K\pi\pi^0$ mode results were obtained by CLEO [10] in the framework of a 7-resonance model (ρ^+ , K^{*-} , \bar{K}^{0*} , $K_0(1430)^-$, $\bar{K}_0(1430)^0$, $\rho(1700)^+$, $K^{*-}(1680)$ and a nonresonant contribution) and the 3-resonance model ($K^{*-}\pi^+$, $\bar{K}^{0*}\pi^0$, $\rho^+\pi^-$, nonresonant $K^-\pi^+\pi^0$). The difference in the resulting efficiency using two different models is treated as a corresponding systematic error. The resulting systematic error due to the decay model uncertainty is 1.8%.

As mentioned above, we use the generic MC shape in the $M(\pi^+\pi^-\pi^0)$ signal region as the default background description (when calculating the central value of $\mathcal{B}(D^0 \rightarrow \pi^+\pi^-\pi^0)$). To estimate the systematic error related to the description of background, we use an alternative function for the background fit. To do so, we extract true $K\pi\pi^0$ events from generic MC reconstructed as $\pi^+\pi^-\pi^0$. The shape obtained (see Fig. 5, right) is fitted with a 2^{nd} order polynomial multiplied by an error function and a 1^{st} order polynomial. We use this parameterization for the misidentification background, while another 1^{st} order polynomial is added to fit the other charm- (other than misidentification), light- and b -quark linear contributions. The difference between this and the default fit (0.4%) is added in quadrature to the systematic error.

To determine the signal fit uncertainty, a different $D^0 \rightarrow \pi^+\pi^-\pi^0$ signal parameterization, composed of two bifurcated Gaussians and one regular Gaussian is used. For the $D^0 \rightarrow K\pi\pi^0$ decay channel we use a bifurcated hyperbolic Gaussian and a regular Gaussian. The relative differences to the default fit are found to be 0.3% and 0.5% for the $\pi^+\pi^-\pi^0$ and $K^-\pi^+\pi^0$ mode, respectively, and are added to the total systematic uncertainty.

Finally, we varied the selection criteria and estimate the systematic error corresponding to the possible inadequate background description. The particle identification selection was changed to $\mathcal{R}_{PID}(\pi) < 0.2$, $\mathcal{R}_{PID}(K) > 0.8$, and the resulting systematic uncertainty is found to be negligible. Change of the $p_{cms}(D^*)$ requirement (3.0 GeV/c) results in a 0.4% error. A significant uncertainty is due to the K_S veto; after excluding the region $0.195 \text{ GeV}^2/c^4 < M^2(\pi^+\pi^-) < 0.305 \text{ GeV}^2/c^4$, the resulting $\pi^+\pi^-\pi^0$ yield changes by 1.6%.

The individual sources of the systematic error are listed in Table II. The total uncertainty is obtained by adding all contributions in quadrature.

TABLE II: Systematic errors

Source	Error, %
MC statistics	0.8
PID efficiency of K/π	1.6
Decay model	1.8
Fit (background & signal)	0.7
$p_{cms}(D^*)$ cut	0.4
K_S^0 veto	1.6
Total	3.1

RESULTS

Summarizing the discussion above, we obtain the following ratio of the branching fractions:

$$\frac{\mathcal{B}(D^0 \rightarrow \pi^+\pi^-\pi^0)}{\mathcal{B}(D^0 \rightarrow K^-\pi^+\pi^0)} = \frac{N_{\pi^+\pi^-\pi^0}}{N_{K^-\pi^+\pi^0}} \cdot \frac{\varepsilon_{K\pi\pi^0}}{\varepsilon_{\pi^+\pi^-\pi^0}} \cdot \frac{r_K}{r_\pi} = 0.0971 \pm 0.0009_{\text{stat}} \pm 0.0030_{\text{syst}}.$$

We multiply the obtained value by the 2006 world average of $\mathcal{B}(D^0 \rightarrow K^-\pi^+\pi^0) = (14.1 \pm 0.5)\%$ [11] to calculate the absolute branching fraction for $D^0 \rightarrow \pi^+\pi^-\pi^0$ decay (see Table III). In a recent study by CLEO [5] the relative branching ratio $\mathcal{B}(D^0 \rightarrow \pi^+\pi^-\pi^0)/\mathcal{B}(D^0 \rightarrow K\pi)$ is measured to be 0.344 ± 0.013 . The comparison of the corresponding values for the absolute branching ratio $\mathcal{B}(D^0 \rightarrow \pi^+\pi^-\pi^0)$ shows that both results are in good agreement within the errors (see Table III).

TABLE III: Values of the absolute branching fraction $\mathcal{B}(D^0 \rightarrow \pi^+\pi^-\pi^0)$ by Belle and CLEO-c.

	$N_{\text{ev.}}$	$\mathcal{B}(D^0 \rightarrow \pi^+\pi^-\pi^0), 10^{-3}$
Belle	22803 ± 203	$13.69 \pm 0.13_{\text{stat}} \pm 0.42_{\text{syst}} \pm 0.49_{\text{norm}}$
CLEO-c	10834 ± 164	$13.2 \pm 0.2_{\text{stat}} \pm 0.5_{\text{syst}} \pm 0.2_{\text{norm}} \pm 0.1_{\text{CPcorr.}}$

Finally, we can compare our measurement of the ratio with the ratio obtained from the latest world average values of $\frac{\mathcal{B}(D^0 \rightarrow \pi^+\pi^-\pi^0)}{\mathcal{B}(D^0 \rightarrow K^-\pi^+\pi^0)}$ and $\mathcal{B}(D^0 \rightarrow \pi^-\pi^+\pi^0)$ [11]. Our result $(9.71 \pm 0.31)\%$ is consistent with the world average one $(9.29 \pm 0.54)\%$ and has better accuracy. By choosing the normalization mode $D^0 \rightarrow K^-\pi^+\pi^0$ we avoid many sources of systematic uncertainty including the π^0 detection efficiency and uncertainty in the tracking efficiency. The PID efficiency partially cancels out.

SUMMARY

Using 357 fb^{-1} of data collected with the Belle detector, the first direct measurement of the relative branching fraction $\mathcal{B}(D^0 \rightarrow \pi^+\pi^-\pi^0)/\mathcal{B}(D^0 \rightarrow K^-\pi^+\pi^0)$ has been performed. Our preliminary result 0.0971 ± 0.0031 is compatible with the world average 0.0929 ± 0.0054 and is more precise. The Belle result differs by $\sim 2.8 \sigma$ from the value recently obtained by BaBar [6]: $0.1059 \pm 0.0006 \pm 0.0013$. The corresponding value of the absolute branching fraction $\mathcal{B}(D^0 \rightarrow \pi^+\pi^-\pi^0)$ is $(13.69 \pm 0.66) \times 10^{-3}$.

Acknowledgments

We thank the KEKB group for the excellent operation of the accelerator, the KEK cryogenics group for the efficient operation of the solenoid, and the KEK computer group and the National Institute of Informatics for valuable computing and Super-SINET network support. We acknowledge support from the Ministry of Education, Culture, Sports, Science, and Technology of Japan and the Japan Society for the Promotion of Science; the Australian

Research Council and the Australian Department of Education, Science and Training; the National Science Foundation of China and the Knowledge Innovation Program of the Chinese Academy of Sciences under contract No. 10575109 and IHEP-U-503; the Department of Science and Technology of India; the BK21 program of the Ministry of Education of Korea, the CHEP SRC program and Basic Research program (grant No. R01-2005-000-10089-0) of the Korea Science and Engineering Foundation, and the Pure Basic Research Group program of the Korea Research Foundation; the Polish State Committee for Scientific Research; the Ministry of Science and Technology of the Russian Federation; the Slovenian Research Agency; the Swiss National Science Foundation; the National Science Council and the Ministry of Education of Taiwan; and the U.S. Department of Energy.

-
- [1] D. Cronin-Hennessy *et al.* (CLEO Collaboration), Phys. Rev. D **72**, 031102 (2005).
 - [2] J.M. Link *et al.* (FOCUS Collaboration), Phys. Lett. B **585**, 200 (2004).
 - [3] F. Buccella, M. Lusignoli, A. Pugliese, Phys. Lett. B **379**, 249 (1996).
 - [4] S. Eidelman *et al.*, Phys. Lett. B **592**, 1 (2004).
 - [5] P. Rubin *et al.* (CLEO Collaboration), Phys. Rev. Lett. **96**, 081802 (2006).
 - [6] B. Aubert *et al.* (BABAR Collaboration), hep-ex/0608009.
 - [7] A. Abashian *et al.* (Belle Collaboration), Nucl. Instrum. and Meth. A **479**, 117 (2002).
 - [8] Z. Natkaniec *et al.* (Belle SVD2 Group), Nucl. Instr. and Meth. A **560**, 1 (2006).
 - [9] GEANT, R. Brun *et al.*, GEANT 3.21, CERN Report DD/EE/84-1, 1984.
 - [10] S. Kopp *et al.* (CLEO Collaboration), Phys. Rev. D **63**, 092001 (2001).
 - [11] W.-M. Yao *et al.*, J. Phys. G **33**, 1 (2006).
 - [12] V.V. Frolov *et al.* (CLEO Collaboration), hep-ex/0306048.
 - [13] The same function for MC is used to fit the data signal peak. The means and the relative normaliza of the constituting Gaussians are fixed to MC, σ 's and the overall normal are left floating.
 - [14] Hyperbolic Gaussian: $f = \frac{2N}{2\sqrt{\pi}\sigma} \alpha \left| \frac{x-x_0}{\sigma} \right| / (y\sqrt{y-\alpha}) \exp(-(y-\alpha))$, $y = \sqrt{\alpha^2 + \alpha(\frac{x-x_0}{\sigma})^2}$, where the parameters of the distribution are N (normalization), x_0 (mean, or peak position), σ (width) and α . $f((\frac{x-x_0}{\sigma})^2 \ll \alpha) \approx \frac{N}{\sqrt{2\pi}\sigma} \exp(-(\frac{x-x_0}{\sigma})^2)$, $f((\frac{x-x_0}{\sigma})^2 \gg \alpha) \approx \frac{N}{\sqrt{\pi}\sigma} \frac{1}{|x-x_0|} \exp(-\sqrt{\alpha} |\frac{x-x_0}{\sigma}|)$.
 - [15] Bifurcated Gaussian: $f = \frac{2N}{\sqrt{2\pi}(\sigma_1+\sigma_2)} \exp(-(\frac{x-x_0}{\sigma})^2)$, $\sigma(x < x_0) = \sigma_1$, $\sigma(x > x_0) = \sigma_2$, the parameters of the distribution are N (normalization), x_0 (peak position), σ_1 and σ_2 (widths).